



Original Article

Liver Congestion Assessed by Hepatic Vein Waveforms in Patients With Heart Failure

Yukiko Sugawara, MD,^a Akiomi Yoshihisa, MD, PhD,^a Shinji Ishibashi,^b Mitsuko Matsuda,^b Yukio Yamadera,^b Himika Ohara, MD,^a Yasuhiro Ichijo, MD, PhD,^a Koichiro Watanabe, MD,^a Yu Hotsuki, MD,^a Fumiya Anzai, MD,^a Yu Sato, MD,^a Yusuke Kimishima, MD,^a Tetsuro Yokokawa, MD, PhD,^a Tomofumi Misaka, MD, PhD,^a Shinya Yamada, MD, PhD,^a Takamasa Sato, MD, PhD,^a Takashi Kaneshiro, MD, PhD,^a Masayoshi Oikawa, MD, PhD,^a Atsushi Kobayashi, MD, PhD,^a and Yasuchika Takeishi, MD, PhD^a

^aDepartment of Cardiovascular Medicine Fukushima Medical University Hospital, Fukushima, Japan

^bDepartment of Clinical Laboratory Medicine, Fukushima Medical University Hospital, Fukushima, Japan

ABSTRACT

Background: It has been reported that the pattern of hepatic vein (HV) waveforms determined by abdominal ultrasonography is useful for the diagnosis of hepatic fibrosis in patients with chronic liver disease. We aim to clarify the clinical implications of HV waveform patterns in patients with heart failure (HF).

Methods: We measured HV waveforms in 350 HF patients, who were then classified into 3 categories based on their waveforms: those with a continuous pattern (C group); those whose V wave ran under the

RÉSUMÉ

Introduction : Nous avons appris que le tracé ondulatoire de la veine hépatique (VH) à l'échographie abdominale est utile au diagnostic de la fibrose hépatique chez les patients atteints d'une maladie chronique du foie. Nous avons pour objectif de clarifier les implications cliniques des tracés ondulatoires de la VH chez les patients atteints d'insuffisance cardiaque (IC).

Méthodes : Nous avons mesuré les ondulations de la VH de 350 patients atteints d'IC et les avons ensuite classifiés en trois catégories

Systemic venous congestion causes multiple organ failure in patients with heart failure (HF).¹ HF-related liver damage or dysfunction assessed by liver functional testing, such as total bilirubin,^{2,3} γ -glutamyl transferase,^{4,5} alkaline phosphatase,^{3,6} and cholinesterase,⁷ or scores such as model of end-stage liver disease excluding INR (MELD-XI) score,⁸⁻¹⁰ non-alcoholic fatty liver disease (NAFLD) fibrosis score,¹¹ and Fibrosis-4 (FIB4) index,¹²⁻¹⁴ are reportedly associated with prognosis. In addition, regarding liver image testing in HF patients, it has been reported that novel liver elastography determined by abdominal ultrasonography is an indicator of liver congestion

due to increased right-sided filling pressure (ie, central venous pressure [CVP]).¹⁵⁻¹⁹ However, measurement of liver elastography requires specific abdominal ultrasonographic equipment and is not easy for cardiologists. However, hepatic vein (HV) waveforms have been reported to be useful in the diagnosis of liver fibrosis in patients with chronic liver disease.²⁰⁻²³ With regard to intrarenal venous congestion, it has recently been reported that Doppler intrarenal venous flow pattern is simply classified by the presence or absence of systolic and diastolic interruption and reflects CVP.²⁴⁻²⁶ These interruptions were associated with an elevated A wave and an elevated V wave in intrarenal venous waveforms, and the elevated V wave was caused by increased CVP and right ventricular dysfunction.

We hypothesized that (1) HV waveforms determined by standard abdominal ultrasonography or echocardiographic equipment can be measured easily compared with liver elastography; (2) HV waveforms have more sensitively measurable CVP than kidneys, as the liver is located closer to the heart than the kidneys; and (3) HV waveforms reflect liver dysfunction. Thus, in this study, we aimed to identify liver congestion using HV waveforms determined by abdominal

Received for publication December 29, 2020. Accepted February 3, 2021.

Ethics Statement: The study protocol was approved by the Ethics Committee of Fukushima Medical University. All patients gave written informed consent.

Corresponding author: Dr Akiomi Yoshihisa, Department of Cardiovascular Medicine, Fukushima Medical University, 1 Hikarigaoka, Fukushima, 960-1295, Japan. Tel.: +81-24-547-1190, fax: +81-24-548-1821.

E-mail: yoshihis@fmu.ac.jp

See page 784 for disclosure information.

baseline (U group), and those with a reversed V wave (R group). We performed right-heart catheterization, and examined the rate of post-discharge cardiac events, such as cardiac death and rehospitalization due to worsening HF.

Results: The number of patients in each of the 3 HV waveform groups was as follows: C group, n = 158; U group, n = 152, and R group, n = 40. The levels of B-type natriuretic peptide (R vs C and U; 245.8 vs 111.7 and 216.6 pg/mL; $P < 0.01$) and mean right atrial pressure (10.5 vs 6.7 and 7.2 mm Hg; $P < 0.01$) were highest in the R group compared with the other groups. The Kaplan-Meier analysis found that cardiac event-free rates were lowest in the R group among all groups (log-rank $P < 0.001$). In the multivariable Cox proportional hazard analysis, the R group was found to be an independent predictor of cardiac events (hazard ratio, 4.90; 95% confidence interval, 2.23-10.74; $P < 0.01$).

Conclusion: Among HF patients, those with reversed V waves had higher right atrial pressure and were at higher risk of adverse prognosis.

Doppler ultrasonography and their prognostic significance in HF patients.

Methods

Subjects and study protocol

This was a prospective observational study. We encouraged patients and attending physicians to perform abdominal ultrasonography to evaluate liver disease or damage in a stable condition before hospital discharge. Of 645 decompensated HF patients who were hospitalized in Fukushima Medical University between April 2018 and March 2020, 388 underwent abdominal ultrasonography. The diagnosis of decompensated HF was made by each patient's attending cardiologist based on the established HF guidelines.²⁷⁻²⁹ Blood samples, abdominal ultrasonography, and echocardiography were obtained at hospital discharge. The patient flow is described in Figure 1. The exclusion criteria included patients who were positive for hepatitis B surface antigen and/or hepatitis C antibody, those with obvious chronic liver diseases (eg, cirrhosis, liver tumors), those who were receiving maintenance dialysis, and those who were lacking or presented with poor HV waveforms. Finally, 350 patients were enrolled in the study. These patients were classified into 3 categories based on their HV waveforms: those with a continuous pattern (C group), those whose V wave ran under the baseline (U group), and those with a reversed V wave (R group).

First, we compared the clinical features and the results from laboratory tests, echocardiography, and right-heart catheterization (RHC) among the 3 groups. Second, the patients were followed up until July 2020 for cardiac events as composites of cardiac death or unplanned rehospitalization for HF treatment. Cardiac death was defined as death from ventricular fibrillation, acute coronary syndromes, or worsening heart failure. For patients who experienced ≥ 2 events,

selon leurs ondulations : ceux qui avaient un tracé continu (groupe C); ceux dont l'onde V se présentait selon les valeurs de référence (groupe U); ceux qui avaient une onde V inversée (groupe R). Nous avons réalisé un cathétérisme cardiaque droit et examiné le taux d'événements cardiaques après la sortie de l'hôpital tels que la mort d'origine cardiaque et la réhospitalisation en raison de l'aggravation de l'IC.

Résultats : Le nombre de patients dans chacun des trois groupes d'ondulations de la VH était réparti comme suit : groupe C, n = 158; groupe U, n = 152 et groupe R, n = 40. Les concentrations en peptides natriurétiques de type B (R vs C et U; 245,8 vs 111,7 et 216,6 pg/ml; $P < 0,01$) et la pression moyenne de l'oreillette droite (10,5 vs 6,7 et 7,2 mmHg; $P < 0.01$) étaient plus élevées dans le groupe R que dans les autres groupes. La méthode de Kaplan-Meier a montré que les taux sans événement cardiaque étaient plus faibles dans le groupe R que dans les autres groupes (P du test logarithmique par rangs $< 0,001$). À l'analyse multivariée selon le modèle à risques proportionnels de Cox, nous avons observé que le groupe R était un prédicteur indépendant des événements cardiaques (rapport de risque, 4,90; intervalle de confiance à 95 %, 2,23-10,74; $P < 0,01$).

Conclusion : Chez les patients atteints d'IC, ceux qui avaient des ondes V inversées avaient une pression plus élevée de l'oreillette droite et étaient exposés à un risque plus élevé de pronostic défavorable.

only the first event was included in the analysis. Because the patients visited the hospital monthly or every other month, we were able to follow up with all patients. Status and dates of death were obtained from the patients' medical records. Those administering the survey were blind to the analyses, and written informed consent was obtained from all study subjects. The study protocol was approved by the Ethics Committee of Fukushima Medical University and was carried out in accordance with the principles outlined in the Declaration of Helsinki. Reporting of the study conforms to the Strengthening the Reporting of Observational Studies in Epidemiology guidelines and the Enhancing the Quality and Transparency of Health Research guidelines.

Abdominal ultrasonography and HV waveforms

All examinations were performed by experienced sonographers, using an Aplio i800 (Canon Medical Systems, Tokyo,

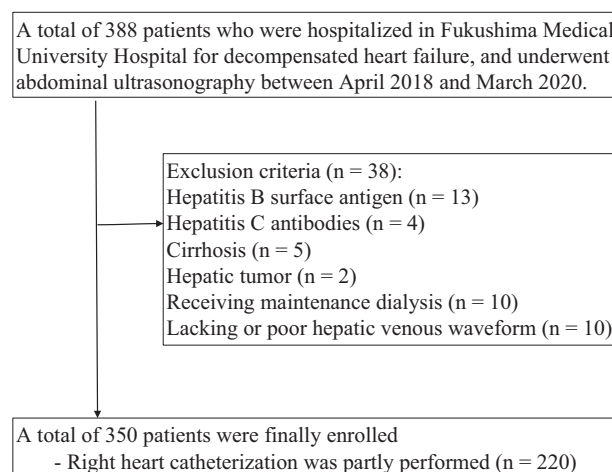
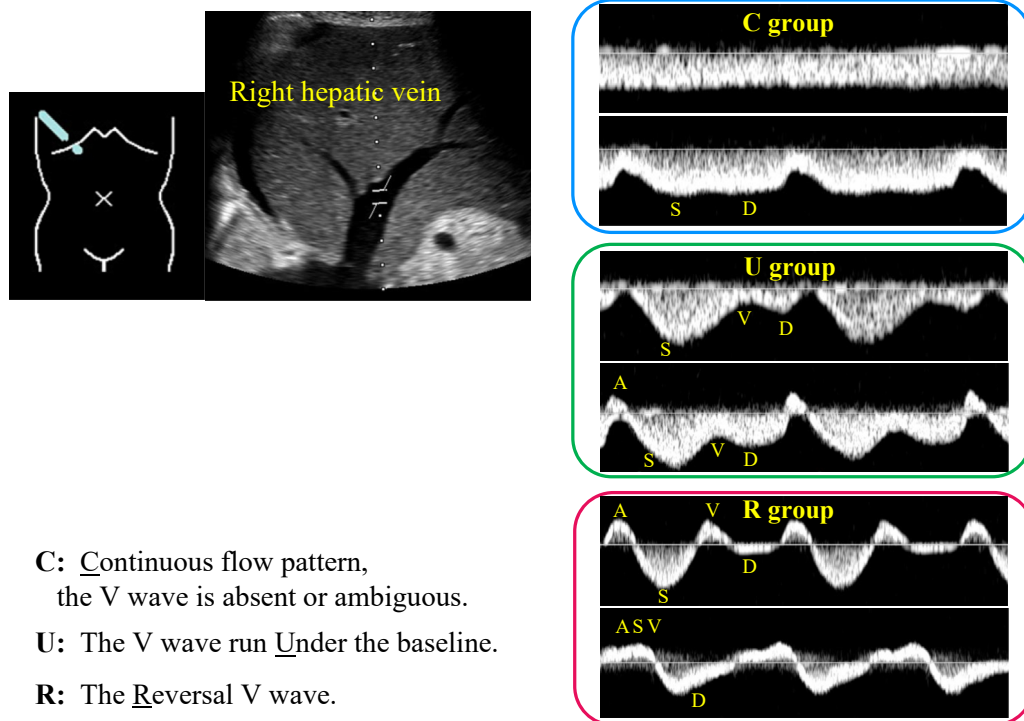


Figure 1. Patient flowchart.



- C:** Continuous flow pattern, the V wave is absent or ambiguous.
- U:** The V wave runs Under the baseline.
- R:** The Reversal V wave.

Figure 2. Classification of hepatic vein waveforms. Continuous flow pattern or ambiguous V wave (C group, n = 158). The V wave runs under the baseline (U group, n = 152). Reversed V wave (R group, n = 40).

Japan) with a 1.8-6.4 MHz convex transducer. HV was identified in reference to continuity with the inferior vena cava (IVC), direction of blood flow, and other identifiers. HV waveforms were obtained using a pulsed-wave Doppler device. The tests were undertaken by approaching the right HV 3-5 cm proximal to the IVC from the right intercostal space (Fig 2). In HF patients with atrial fibrillation, HV waveforms were measured during 5 relatively stable beats. In patients with atrial fibrillation, the C wave was used instead of the A wave.^{20,25} Based on previous studies,²⁰⁻²³ we focused on the shapes and positions of the V wave. We classified HV waveforms in accordance with the shape and position of the V wave into 3 patterns (Fig 2) and divided the total 350 HF patients into 3 groups: those in whom the continuous flow pattern or V wave was ambiguous (C group), those in whom the V wave ran under the baseline (U group), and those who had a reversed V wave (R group). The inter- and intraobserver variability of the HV waveforms classification was proven by using Cohen's kappa method.

Echocardiography

Echocardiography was performed blindly by experienced echocardiographers using standard techniques.³⁰ Echocardiographic parameters such as left ventricular ejection fraction, right atrium area, right ventricular area, IVC diameter, tricuspid regurgitation pressure gradient, and tricuspid annular plane systolic excursion were measured. Left ventricular ejection fraction was calculated using Simpson's method.

RHC

RHC was partly performed in 220 patients based on the remedial judgment of the attending physician (eg,

hemodynamic assessment in conjunction with an evaluation of coronary artery disease, valvular disease, myocardial disease, or arrhythmia) within 3 days of abdominal ultrasonography. RHC was performed with the patients in a stable condition, in a resting supine position under fluoroscopic guidance, at room temperature, and at rest using a 7F Swan-Ganz catheter (Edwards Lifesciences, Irvine, CA).^{11,19} Cardiac output was calculated based on the thermodilution method.

Statistical methods

Normally distributed data are presented as mean \pm standard deviation, and nonnormally distributed data are presented as median (25th percentile, 75th percentile). The characteristics of the 3 groups were compared using analysis of variance, Kruskal-Wallis tests, and χ^2 tests depending on the type and distribution of the data. Kaplan-Meier analysis was used with a log-rank test to assess cardiac event rates. Cox proportional hazard analyses were used to evaluate HV waveforms as predictors of cardiac events, and were adjusted for general confounding factors in HF patients (ie, age, sex, hemoglobin, creatinine, B-type natriuretic peptide, left ventricular ejection fraction, IVC, and tricuspid regurgitation pressure gradient). A *P* value of < 0.05 was considered statistically significant for all comparisons. These analyses were performed using a statistical software package (SPSS version 27.0, IBM, Armonk, NY).

Results

Of 645 decompensated HF patients, 388 (60.2%) underwent abdominal ultrasonography, and 350 (54.3%) were finally enrolled. The number of patients in each of the 3 HV

Table 1. Baseline patient characteristics (N = 360)

	C group (n = 158)	U group (n = 152)	R group (n = 40)	P value
Demographics				
Age (y)	68.5 ± 14.1	68.8 ± 13.1	68.5 ± 14.8	0.97
Male sex (n, %)	90 (60.0)	87 (57.2)	27 (67.5)	0.45
Body mass index (kg/m ²)	23.3 ± 4.4	22.7 ± 3.9	23.1 ± 3.7	0.34
NYHA class III or IV	40 (25.3)	39 (25.6)	18 (45.0)	0.26
Etiology	25 (15.8)/32 (20.3)/47 (29.7)/16 (10.1)/15 (9.5)/4 (2.5)/18 (11.3)	25 (16.4)/39 (25.7)/44 (43.6)/11 (7.2)/17 (11.2)/2 (1.3)/13 (8.5)	8 (20.0)/10 (25.0)/10 (9.9)/3 (7.5)/3 (7.5)/ 2 (5.0)/4 (10.0)	0.81
Ischemic/myopathy/valvular/arrhythmia/pulmonary/congenital/others				
Comorbidities				
CAD (n, %)	38 (24.0)	38 (25.0)	15 (37.5)	0.21
Atrial fibrillation (n, %)	54 (34.2)	55 (36.2)	15 (37.5)	0.90
Hypertension (n, %)	105 (66.5)	94 (61.8)	23 (57.5)	0.50
Dyslipidemia (n, %)	110 (69.6)	91 (59.9)	30 (75.0)	0.09
Diabetes mellitus (n, %)	54 (34.2)	55 (36.2)	20 (50.0)	0.18
CKD (n, %)	91 (57.6)	96 (63.2)	25 (62.5)	0.58
Anemia (n, %)	76 (48.1)	72 (47.3)	22 (55.0)	0.68
Laboratory data				
Hemoglobin (g/dL)	13.1 (11.6-14.6)	12.8 (11.3-14.5)	12.3 (11.2-14.1)	0.25
Total bilirubin (mg/dL)	0.7 (0.6-1.0)	0.8 (0.6-1.0)	0.9 (0.7-1.3)*	0.03
Aspartate aminotransferase (U/L)	22.0 (17.0-28.0)	23.0 (19.0-28.0)	24.5 (18.3-32.0)	0.30
Alanine aminotransferase (U/L)	19.0 (13.0-28.0)	18.0 (13.0-27.0)	17.0 (10.0-25.3)	0.46
Alkaline phosphatase (U/L)	234.0 (184.0-280.0)	251.5 (197.5-307.5)	280.0 (183.7-344.8)	0.07
Gamma-glutamyl transferase (U/L)	35.0 (18.0-63.0)	39.0 (21.0-80.3)	39.0 (26.0-118.5)	0.11
BNP (pg/mL)	111.7 (57.6-264.8)	216.6 (98.7-489.5)†	245.8 (157.0-553.5)‡	< 0.01
Creatinine (mg/dL)	1.0 (0.8-1.2)	1.0 (0.8-1.2)	1.0 (0.9-1.4)	0.27
Echocardiography				
LV ejection fraction (%)	50.5 ± 16.6	48.3 ± 17.1	48.6 ± 17.7	0.49
RA end systolic area (cm ²)	18.7 ± 7.5	20.4 ± 9.0	23.4 ± 9.7	0.08
RV area diastole (cm ²)	21.0 ± 7.8	21.0 ± 8.4	22.8 ± 8.2	0.83
RV area systole (cm ²)	13.9 ± 6.8	13.7 ± 7.4	15.4 ± 7.9	0.83
RV fractional area change (%)	36.6 ± 10.4	35.7 ± 12.1	34.4 ± 12.0	0.71
IVC diameter (mm)	14.3 ± 3.8	16.5 ± 4.7†	18.9 ± 5.6†,‡	< 0.01
TRPG (mm Hg)	26.5 ± 10.7	28.5 ± 13.8	32.3 ± 18.0	0.06
Moderate or severe TR (n, %)	12 (7.5)	16 (10.5)	4 (10.0)	0.66
Tricuspid valve S' (cm)	10.1 ± 2.9	8.9 ± 2.7	8.7 ± 2.0	0.22
TAPSE (cm)	17.9 ± 4.2	17.3 ± 4.8	17.1 ± 5.0	0.51
Right heart catheterisation				
Pulmonary arterial wedge pressure (mm Hg)	14.0 ± 7.5	15.1 ± 7.4	19.2 ± 6.0†	0.01
Mean pulmonary artery pressure (mm Hg)	24.0 ± 9.1	25.7 ± 10.7	33.0 ± 10.4†,‡	< 0.01
Transpulmonary pressure gradient (mm Hg)	10.0 ± 7.7	10.6 ± 8.8	13.7 ± 8.7	0.17
Mean right atrium pressure (mm Hg)	6.7 ± 3.4	7.2 ± 3.6	10.5 ± 5.4†,‡	< 0.01
Cardiac index (L/min/m ²)	2.5 ± 0.6	2.5 ± 0.8	2.4 ± 0.6	0.63
Medical therapy				
β-blockers (n, %)	115 (72.8)	104 (68.4)	25 (62.5)	0.40
RAS inhibitors (n, %)	107 (67.7)	96 (63.2)	23 (57.5)	0.43
Inotropic agents (n, %)	17 (10.8)	14 (9.2)	5 (12.5)	0.80
Diuretics (n, %)	96 (60.8)	101 (66.4)	29 (72.5)	0.31

BNP, B-type natriuretic peptide; CAD, coronary artery disease; C group, continuous flow patterns; CKD, chronic kidney disease; IVC, inferior vena cava; LV, left ventricular; NYHA, New York Heart Association; RA, right atrial; RAS, renin-angiotensin system; R group, the reversed V wave; RV, right ventricular; TAPSE, tricuspid annular plane systolic excursion; TR, tricuspid regurgitation; TRPG, tricuspid regurgitation pressure gradient; U, the V wave under the baseline.

vs C.

* $P < 0.05$.

† $P < 0.01$ vs U.

‡ $P < 0.01$ after the Bonferroni correction.

waveform groups was as follows: C group, n = 158; U group, n = 152, and R group, n = 40. Regarding assessment of HV waveforms, the kappa value of interobserver variability was 0.85 and intraobserver reproducibility was 0.92. The comparisons of patient characteristics among the 3 groups are summarized in Table 1. There were no significant differences in age, sex, body mass index, HF etiology, or comorbidities among the 3 groups. Regarding laboratory data, there were no significant differences in the levels of liver function testing,

including aspartate aminotransferase, alanine aminotransferase, alkaline phosphatase, gamma-glutamyl transferase, and cholinesterase, except for total bilirubin (0.9 vs 0.7 and 0.8 mg/dL; $P = 0.03$). In contrast, levels of B-type natriuretic peptide were highest in the R groups (245.8 vs 111.7 and 216.6 pg/mL; $P < 0.01$). With respect to the echocardiographic parameters, all echocardiographic parameters, except for IVC diameter (18.9 vs. 14.3 and 16.5 mm, $P < 0.01$), were comparable among the groups. With regard to RHC,

pulmonary arterial wedge pressure (19.2 vs 14.0 and 15.1 mm Hg; $P = 0.012$), mean pulmonary arterial pressure (33.0 vs 24.0 and 25.7 mm Hg; $P < .001$), and mean right atrial pressure (10.5 vs 6.7 and 7.2 mm Hg; $P < 0.01$) were highest in the R group. In contrast, transpulmonary pressure gradient and cardiac index did not significantly differ among the groups.

During the follow-up period of a median of 304 days (range, 6-824 days), 50 cardiac events occurred, including 45 rehospitalizations due to worsening heart failure and 5 cardiac deaths. The Kaplan-Meier analysis (Fig 3) showed that the cardiac event-free rate was lowest in the R group among the groups (log-rank $P < 0.001$). In addition, cardiac event-free rates were lowest in the R group among all groups, regardless of the presence or absence of atrial fibrillation (Fig 4; log-rank $P < 0.001$, respectively). In the multivariable Cox proportional hazard analysis, the presence of a reversed V wave was found to be an independent predictor of cardiac events (Table 2; hazard ratio, 4.90; 95% confidence interval, 2.23-10.74; $P < 0.01$).

Discussion

This study is the first to report that the HV waveforms with the reversed V wave pattern (R group) are associated with higher levels of B-type natriuretic peptide and increased CVP (higher mean atrium pressure and IVC diameter), rather than liver dysfunction, and with higher cardiac event rates in HF patients.

HV waveforms are reported to be useful for the diagnosis of liver fibrosis in patients with chronic liver disease.²⁰⁻²³ Although several classifications of HV waveforms have been reported, there is no established classification with universally accepted evidence,²⁰⁻²³ and their association with hemodynamics in HF patients has, to date, not been examined. A normal HV waveform is a 3-phase waveform consisting of 4 waves: retrograde A wave, antegrade S wave, transition V wave, and antegrade D wave.^{20,25,31} The A wave is caused by an increase in right atrial pressure, which itself is caused by the atrial contraction that occurs at the end of the diastole.²⁰ The S wave is a decreasing of right atrial pressure, caused by sucking, which is the inflow to the right atrium as the atrioventricular septum descends during early- to mid-systole.²⁰ The V wave represents an increase in right atrial pressure that occurs during continued systemic venous return to the closed tricuspid valve. At the opening of the tricuspid valve and the transition from systole to diastole, the wave peaks and shifts to the D wave.²⁰ The lowest point of the D wave is the maximum diastolic flow velocity. The V wave corresponds to atrial overfilling.²⁰ The blood flow to the heart appears below the baseline, and the reversed blood flow to the liver from the heart appears above the baseline. After the end systole, as the ventricular contraction intensity decreases and the closed tricuspid valve begins to return to its original resting position, the atrium fills, blood flow velocity (from the liver to the heart) decreases, and temporary equilibrium is reached, making V waves.²⁰ Therefore, the greater congestion and right atrial volume overload at the end of systole leads to deeper reversed V waves. The S wave is smaller in patients with high

CVP and right ventricular pressure overload, and if the A, S, and V waves are all retrograde, they may fuse into a single retrograde wave and become biphasic waveforms, alternating with the D wave.^{20,21} In patients with severe tricuspid regurgitation, systolic reverse flow in HV is sometimes observed, depending on right ventricular function and right atrial compliance.^{20,21,32} From these reports, in this study, we divided the HV waveforms into 3 categories according to the position of the V wave above or below the baseline as a new classification. Similar to previous reports regarding renal congestion,²⁴⁻²⁶ Doppler HV waveforms in this study were found to be associated with CVP. However, measurement of HV waveforms seemed to be superior to those of intrarenal venous flow pattern, in terms of ease of measurement and accuracy of CVP, because of their closer anatomic proximity to the heart. In addition, contrary to our expectations, Doppler HV waveforms were not associated with liver function testing. However, this study's relatively small sample size may have affected the statistical significance.

With regard to the HV waveforms, it has been suggested that the significance of HV waveforms differ depending on the disease.^{20,33} In patients with chronic liver disease, HV waveforms are useful for the estimation of liver fibrosis.²⁰⁻²³ In patients with liver cirrhosis, the continuous HV waveform (namely C group in this study) is mainly caused by intrahepatic fat deposition, inflammatory or fibrotic changes, and changes in the compliance of the venous wall, suggesting the presence of severe liver fibrosis.³⁴⁻³⁶ In postoperative Fontan patients with right-sided HF, liver fibrosis is caused by long-lasting liver congestion, and the HV waveform tends to be a monophasic and continuous waveform (C group in this study) with increased CVP.^{22,37,38} Contrary to the above-mentioned results,^{22,37,38} HF patients with increased CVP present with a reversed V wave pattern (R group in this study). Although we could not fully explain the reason for this discrepancy, the lack of distinct liver disease or severe liver fibrosis might have had an effect. Therefore, the results of this study are in contrast to those of previous studies^{22,37,38} on HV waveform classification in patients with liver cirrhosis.

In addition, it was reported recently that the ratio of the S and D wave amplitudes of HV waveforms is useful for the diagnosis of cardiac disease (eg, right-sided HF, tricuspid regurgitation, pulmonary hypertension).^{20,21} The S wave becomes smaller or retrograde waves mixed with the A waves and V waves (similar to R group in this study) in patients with high CVP and right ventricular pressure overload.^{21,39} However, it may be difficult to define the ratio of the amplitudes of the S and D waves in all cases. In the case of antegrade S waves, the S/D wave ratio could be predictive of CVP. We here report the utility of a simple HV waveform pattern, which needs neither measurement nor calculation, for estimating RAP and prognosis.

It has been reported that IVC diameter and collapsibility index are related to right atrial pressure^{27,40,41} and prognosis in HF patients.⁴² Concordant with the results of previous studies,^{27,40-42} the IVC diameter in this study was larger, and right atrial pressure was higher in the R group and was associated with worse prognosis. However, it remains controversial whether IVC diameter indicates right atrial pressure or

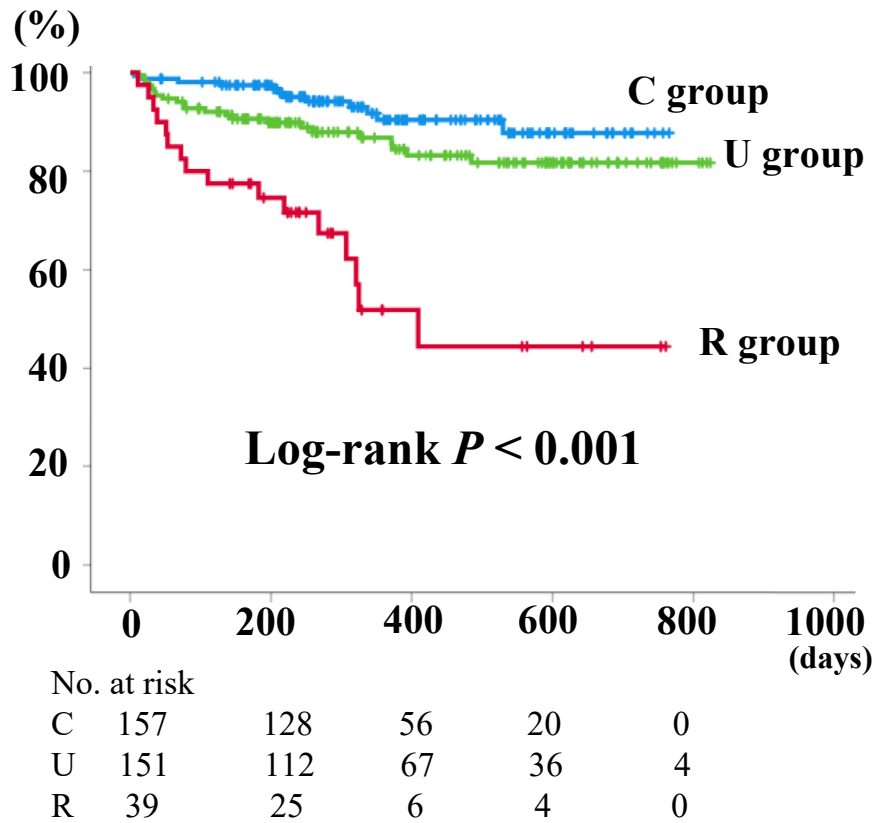


Figure 3. Accumulated event-free rates stratified by hepatic vein waveforms. C, continuous flow patterns group; R, the reversal V wave group; U, the V wave under the baseline group.

prognosis in HF patients,⁴³⁻⁴⁵ and cutoff of collapsibility of IVC diameter has been unestablished.^{40,41,46} Implantable hemodynamic monitors are accurate alternatives to RHC⁴⁷⁻⁴⁹ and are potentially useful to avoid rehospitalization due to worsened HF^{50,51} because increases in intracardiac and pulmonary arterial pressure precede clinical decompensation.^{52,53}

However, these sensors are invasive, and noninvasive hemodynamic indicators are required for daily clinical settings. In this regard, lung ultrasonography can detect lung congestion and left atrial pressure⁵⁴ and shows moderate correlation with RHC.⁵⁵ Similarly, abdominal ultrasonography is readily accessible and easy to perform. Therefore, HV waveforms can

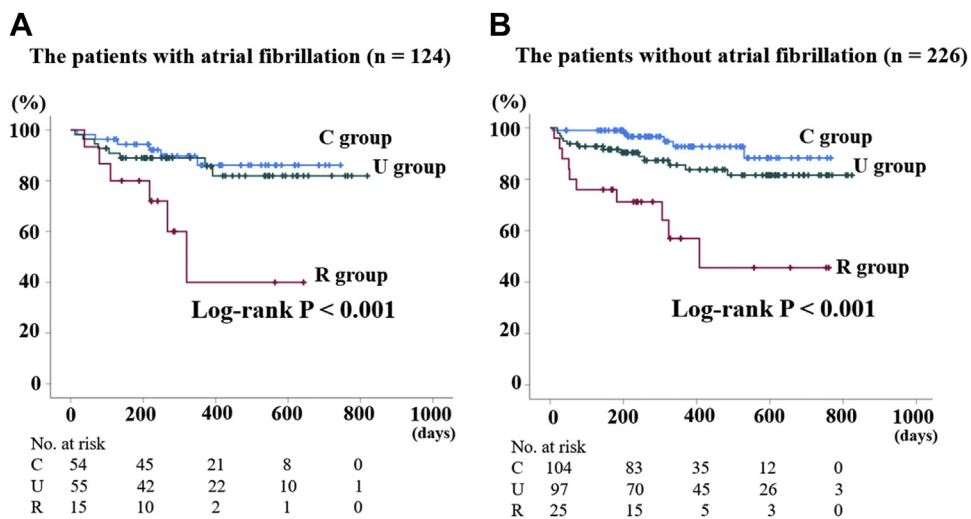


Figure 4. Accumulated event-free rates stratified by hepatic vein waveforms in all patients. (A) Patients with atrial fibrillation. (B) Patients without atrial fibrillation. C, continuous flow patterns group; R, the reversal V wave group; U, the V wave under the baseline group.

Table 2. Cox proportional hazard analysis for cardiac event (event n = 50/360)

	HR	95% CI	P value
R vs C (unadjusted)	6.79	3.21-14.40	< 0.01
R vs C (Model 1)	6.64	3.12-14.16	< 0.01
R vs C (Model 2)	4.90	2.23-10.74	< 0.01
R vs C (Model 3)	7.81	4.00-19.7	< 0.01
R vs U (unadjusted)	3.59	1.87-6.87	< 0.01
R vs U (Model 1)	3.53	1.84-6.81	< 0.01
R vs U (Model 2)	3.58	1.86-6.90	< 0.01
R vs U (Model 3)	3.25	1.61-6.60	< 0.01
U vs C (unadjusted)	1.88	0.930-3.803	0.08

Model 1: adjusted for age and sex. Model 2: adjusted for Model 1, hemoglobin, creatinine, B-type natriuretic peptide, and left ventricular ejection fraction. Model 3: adjusted for Model 1, IVC diameter, and tricuspid regurgitation pressure gradient.

C, continuous flow patterns group; CI, confidence interval; HR, hazard ratio; R, the reversal V wave group; U, the V wave under the baseline group.

be helpful in the noninvasive estimation of right atrial pressure and prognosis.

Limitations

First, because of the prospective study design and small sample size, the study might be underpowered. However, study population of this study was much larger than those of previous studies.^{21,22,33,56} Second, although documented liver disease was excluded in this study, we could not fully exclude the presence of subsequent liver diseases, which may have affected the HV waveforms. Third, the relationships between HV waveforms and other estimations, such as liver biopsy, or other imaging, such as computed tomography and magnetic resonance imaging, were not examined in this study. Fourth, we used clinical variables obtained during hospitalization, without considering changes in HV waveforms, other parameters, or treatments after discharge. Fifth, although we encouraged abdominal ultrasonography, we could not perform it in all patients for various reasons (e.g. patient refusal). Additionally, whether RHC was to be performed was decided by each patient's attending physician. There might be potential selection bias of patients. Sixth, we did not evaluate the S/D ratio of HV and IVC collapsibility in the present study.^{40,41} Therefore, further studies with larger populations are needed.

Conclusion

Among HF patients, those with reversed V waves had higher right atrial pressure and were at higher risk of adverse prognosis.

Acknowledgements

The authors thank Ms. Tomiko Miura, Ms. Kumiko Watanabe, and Ms. Yumi Yoshihisa for their technical assistance.

Funding Sources

This work was supported in part by a grant-in-aid for Scientific Research (No. 20K07828) from the Japan Society for the Promotion of Science, Tokyo, Japan.

Disclosures

Akiomi Yoshihisa and Tomofumi Misaka belong to the Department of Advanced Cardiac Therapeutics, which is supported by Fukuda-Denshi Co, Ltd. Tetsuro Yokokawa and Koichi Sugimoto belong to the Department of Pulmonary Hypertension, which is supported by ACTELION PHARMA Co, Ltd. These companies are not associated with the contents of this study. The other authors have no conflicts of interest to disclose.

References

- Verbrugge FH, Dupont M, Steels P, et al. Abdominal contributions to cardiorenal dysfunction in congestive heart failure. *J Am Coll Cardiol* 2013;62:485-95.
- Allen LA, Felker GM, Pocock S, et al. Liver function abnormalities and outcome in patients with chronic heart failure: data from the Candesartan in Heart Failure: Assessment of Reduction in Mortality and Morbidity (CHARM) program. *Eur J Heart Fail* 2009;11:170-7.
- Samsky MD, Patel CB, DeWald TA, et al. Cardiohepatic interactions in heart failure: an overview and clinical implications. *J Am Coll Cardiol* 2013;61:2397-405.
- Poelzl G, Eberl C, Achraimer H, et al. Prevalence and prognostic significance of elevated gamma-glutamyltransferase in chronic heart failure. *Circ Heart Fail* 2009;2:294-302.
- Ruttman E, Brant LJ, Concin H, Diem G, Rapp K, Ulmer H. Gamma-glutamyltransferase as a risk factor for cardiovascular disease mortality: an epidemiological investigation in a cohort of 163,944 Austrian adults. *Circulation* 2005;112:2130-7.
- Poelzl G, Ess M, Mussner-Seeber C, Pachinger O, Frick M, Ulmer H. Liver dysfunction in chronic heart failure: prevalence, characteristics and prognostic significance. *Eur J Clin Invest* 2012;42:153-63.
- Sato T, Yamauchi H, Suzuki S, et al. Serum cholinesterase is an important prognostic factor in chronic heart failure. *Heart Vessels* 2015;30:204-10.
- Abe S, Yoshihisa A, Takiguchi M, et al. Liver dysfunction assessed by model for end-stage liver disease excluding INR (MELD-XI) scoring system predicts adverse prognosis in heart failure. *PLoS One* 2014;9:e100618.
- Biegus J, Demissei B, Postmus D, et al. Hepatorenal dysfunction identifies high-risk patients with acute heart failure: insights from the RELAX-AHF trial. *ESC Heart Fail* 2019;6:1188-98.
- Okano T, Motoki H, Minamisawa M, et al. Cardio-renal and cardio-hepatic interactions predict cardiovascular events in elderly patients with heart failure. *PLoS One* 2020;15:e0241003.
- Yoshihisa A, Sato Y, Yokokawa T, et al. Liver fibrosis score predicts mortality in heart failure patients with preserved ejection fraction. *ESC Heart Fail* 2018;5:262-70.
- So-Armah KA, Lim JK, Lo Re V 3rd, et al. FIB-4 stage of liver fibrosis is associated with incident heart failure with preserved, but not reduced, ejection fraction among people with and without HIV or hepatitis C. *Prog Cardiovasc Dis* 2020;63:184-91.
- Iwasaki Y, Tomiyama H, Shiina K, et al. Liver stiffness and arterial stiffness/abnormal central hemodynamics in the early stage of heart failure. *Int J Cardiol Heart Vasc* 2018;20:32-7.
- Sato Y, Yoshihisa A, Kanno Y, et al. Liver stiffness assessed by Fibrosis-4 index predicts mortality in patients with heart failure. *Open Heart* 2017;4:e000598.

15. Taniguchi T, Ohtani T, Kioka H, et al. Liver stiffness reflecting right-sided filling pressure can predict adverse outcomes in patients with heart failure. *JACC Cardiovasc Imaging* 2019;12:955-64.
16. Taniguchi T, Sakata Y, Ohtani T, et al. Usefulness of transient elastography for noninvasive and reliable estimation of right-sided filling pressure in heart failure. *Am J Cardiol* 2014;113:552-8.
17. Colli A, Pozzoni P, Berzuini A, et al. Decompensated chronic heart failure: increased liver stiffness measured by means of transient elastography. *Radiology* 2010;257:872-8.
18. Soloveva A, Kobalava Z, Fudim M, et al. Relationship of liver stiffness with congestion in patients presenting with acute decompensated heart failure. *J Card Fail* 2019;25:176-87.
19. Yoshihisa A, Ishibashi S, Matsuda M, et al. Clinical implications of hepatic hemodynamic evaluation by abdominal ultrasonographic imaging in patients with heart failure. *J Am Heart Assoc* 2020;9:e016689.
20. Scheinfeld MH, Bilali A, Koenigsberg M. Understanding the spectral Doppler waveform of the hepatic veins in health and disease. *Radiographics* 2009;29:2081-98.
21. Sun DD, Hou CJ, Yuan LJ, Duan YY, Hou Y, Zhou FP. Hemodynamic changes of the middle hepatic vein in patients with pulmonary hypertension using echocardiography. *PLoS One* 2015;10:e0121408.
22. Nakatsuka T, Soroida Y, Nakagawa H, et al. Identification of liver fibrosis using the hepatic vein waveform in patients with Fontan circulation. *Hepatol Res* 2019;49:304-13.
23. McNaughton DA, Abu-Yousef MM. Doppler US of the liver made simple. *Radiographics* 2011;31:161-88.
24. Yamamoto M, Seo Y, Iida N, et al. Prognostic impact of changes in intrarenal venous flow pattern in patients with heart failure. *J Card Fail* 2021;27:20-8.
25. Seo Y, Iida N, Yamamoto M, Ishizu T, Ieda M, Ohte N. Doppler-derived intrarenal venous flow mirrors right-sided heart hemodynamics in patients with cardiovascular disease. *Circ J* 2020;84:1552-9.
26. Iida N, Seo Y, Sai S, et al. Clinical implications of intrarenal hemodynamic evaluation by Doppler ultrasonography in heart failure. *JACC Heart Failure* 2016;4:674-82.
27. Ponikowski P, Voors AA, Anker SD, et al. 2016 ESC Guidelines for the diagnosis and treatment of acute and chronic heart failure: The Task Force for the diagnosis and treatment of acute and chronic heart failure of the European Society of Cardiology (ESC) developed with the special contribution of the Heart Failure Association (HFA) of the ESC. *Eur Heart J* 2016;37:2129-200.
28. Writing Committee M, Yancy CW, Jessup M, et al. 2013 ACCF/AHA guideline for the management of heart failure: a report of the American College of Cardiology Foundation/American Heart Association Task Force on practice guidelines. *Circulation* 2013;128:e240-327.
29. Tsutsui H, Isebe M, Ito H, et al. JCS 2017/JHFS 2017 Guideline on diagnosis and treatment of acute and chronic heart failure—digest version. *Circ J* 2019;83:2084-184.
30. Yoshihisa A, Sato Y, Kanno Y, et al. Prognostic impacts of changes in left ventricular ejection fraction in heart failure patients with preserved left ventricular ejection fraction. *Open Heart* 2020;7:e001112.
31. Lim AK, Patel N, Eckersley RJ, et al. Can Doppler sonography grade the severity of hepatitis C-related liver disease? *AJR Am J Roentgenol* 2005;184:1848-53.
32. Hahn RT, Thomas JD, Khalique OK, Cavalcante JL, Praz F, Zoghbi WA. Imaging assessment of tricuspid regurgitation severity. *JACC Cardiovasc Imaging* 2019;12:469-90.
33. Fadel BM, Alassas K, Husain A, Dahdouh Z, Di Salvo G. Spectral Doppler of the hepatic veins in noncardiac diseases: what the echocardiographer should know. *Echocardiography* 2015;32:1424-7.
34. Bolondi L, Li Bassi S, Gaiani S, et al. Liver cirrhosis: changes of Doppler waveform of hepatic veins. *Radiology* 1991;178:513-6.
35. Karabulut N, Kazil S, Yagci B, Sabir N. Doppler waveform of the hepatic veins in an obese population. *Eur Radiol* 2004;14:2268-72.
36. Dietrich CF, Lee JH, Gottschalk R, et al. Hepatic and portal vein flow pattern in correlation with intrahepatic fat deposition and liver histology in patients with chronic hepatitis C. *AJR Am J Roentgenol* 1998;171:437-43.
37. Munsterman ID, Duijnhouwer AL, Kendall TJ, et al. The clinical spectrum of Fontan-associated liver disease: results from a prospective multimodality screening cohort. *Eur Heart J* 2019;40:1057-68.
38. Wu FM, Opatowsky AR, Raza R, et al. Transient elastography may identify Fontan patients with unfavorable hemodynamics and advanced hepatic fibrosis. *Congenit Heart Dis* 2014;9:438-47.
39. Wells ML, Fenstad ER, Poterucha JT, et al. Imaging findings of congestive hepatopathy. *RadioGraphics* 2016;36:1024-37.
40. Moreno FL, Hagan AD, Holmen JR, Pryor TA, Strickland RD, Castle CH. Evaluation of size and dynamics of the inferior vena cava as an index of right-sided cardiac function. *Am J Cardiol* 1984;53:579-85.
41. Magnino C, Omedè P, Avenatti E, et al. Inaccuracy of right atrial pressure estimates through inferior vena cava indices. *Am J Cardiol* 2017;120:1667-73.
42. Pellicori P, Carubelli V, Zhang J, et al. IVC diameter in patients with chronic heart failure: relationships and prognostic significance. *JACC Cardiovasc Imaging* 2013;6:16-28.
43. Blehar DJ, Resop D, Chin B, Dayno M, Gaspari R. Inferior vena cava displacement during respirophasic ultrasound imaging. *Crit Ultrasound J* 2012;4:18.
44. Simonson JS, Schiller NB. Sonospirometry: a new method for noninvasive estimation of mean right atrial pressure based on two-dimensional echographic measurements of the inferior vena cava during measured inspiration. *J Am Coll Cardiol* 1988;11:557-64.
45. Wallace DJ, Allison M, Stone MB. Inferior vena cava percentage collapse during respiration is affected by the sampling location: an ultrasound study in healthy volunteers. *Acad Emerg Med* 2010;17:96-9.
46. Darwish OS, Mahayni A, Kataria S, Zuniga E, Zhang L, Amin A. Diagnosis of acute heart failure using inferior vena cava ultrasound: systematic review and meta-analysis. *J Ultrasound Med* 2020;39:1367-78.
47. Magalski A, Adamson P, Gadler F, et al. Continuous ambulatory right heart pressure measurements with an implantable hemodynamic monitor: a multicenter, 12-month follow-up study of patients with chronic heart failure. *J Card Fail* 2002;8:63-70.
48. Verdejo HE, Castro PF, Concepcion R, et al. Comparison of a radiofrequency-based wireless pressure sensor to swan-ganz catheter and echocardiography for ambulatory assessment of pulmonary artery pressure in heart failure. *J Am Coll Cardiol* 2007;50:2375-82.
49. Ritzema J, Melton IC, Richards AM, et al. Direct left atrial pressure monitoring in ambulatory heart failure patients: initial experience with a new permanent implantable device. *Circulation* 2007;116:2952-9.

50. Abraham WT, Adamson PB, Bourge RC, et al. Wireless pulmonary artery haemodynamic monitoring in chronic heart failure: a randomised controlled trial. *Lancet* 2011;377:658-66.
51. Adamson PB, Abraham WT, Bourge RC, et al. Wireless pulmonary artery pressure monitoring guides management to reduce decompensation in heart failure with preserved ejection fraction. *Circ Heart Fail* 2014;7:935-44.
52. Zile MR, Bennett TD, St John Sutton M, et al. Transition from chronic compensated to acute decompensated heart failure: pathophysiological insights obtained from continuous monitoring of intracardiac pressures. *Circulation* 2008;118:1433-41.
53. Adamson PB, Magalski A, Braunschweig F, et al. Ongoing right ventricular hemodynamics in heart failure: clinical value of measurements derived from an implantable monitoring system. *J Am Coll Cardiol* 2003;41:565-71.
54. Maw AM, Hassanin A, Ho PM, et al. Diagnostic accuracy of point-of-care lung ultrasonography and chest radiography in adults with symptoms suggestive of acute decompensated heart failure: a systematic review and meta-analysis. *JAMA Netw Open* 2019;2:e190703.
55. Platz E, Lattanzi A, Agbo C, et al. Utility of lung ultrasound in predicting pulmonary and cardiac pressures. *Eur J Heart Fail* 2012;14:1276-84.
56. Acar E, Izci S, Inanir M, et al. Hepatic venous Doppler assessment can anticipate simplified pulmonary embolism severity index and right ventricle dysfunction in patients with acute pulmonary embolism. *J Clin Ultrasound* 2020;48:254-62.